AIP | Review of Scientific Instruments

Development of a multipurpose vacuum chamber for serial optical and diffraction experiments with free electron laser radiation

I. Rajkovic, J. Hallmann, S. Grübel, R. More, W. Quevedo, M. Petri, and S. Techert

Citation: Review of Scientific Instruments **81**, 045105 (2010); doi: 10.1063/1.3327816
View online: http://dx.doi.org/10.1063/1.3327816
View Table of Contents: http://scitation.aip.org/content/aip/journal/rsi/81/4?ver=pdfcov
Published by the AIP Publishing

Development of a multipurpose vacuum chamber for serial optical and diffraction experiments with free electron laser radiation

I. Rajkovic, J. Hallmann, S. Grübel, R. More, W. Quevedo, M. Petri, and S. Techert[a)]
Department of Structural Dynamics of (Bio)chemical Systems, Max Planck Institute for Biophysical Chemistry, 37070 Göttingen, Germany

(Received 3 September 2009; accepted 29 January 2010; published online 12 April 2010)

In this paper we present a development of a multipurpose vacuum chamber which primal function is to be used in pump/probe experiments with free electron laser (FEL) radiation. The chamber is constructed for serial diffraction and serial spectroscopy allowing a fast exchange of samples during the measurement process. For the fast exchange of samples, liquid jet systems are used. Both applications, utilizing soft x-ray FEL pulses as pump and optical laser pulses as probe and vice versa are documented. Experiments with solid samples as well as the liquid jet samples are presented. When working with liquid jets, a system of automatically refilled liquid traps for capturing liquids has been developed in order to ensure stable vacuum conditions. Differential pumping stages are placed in between the FEL beamline and the experimental chamber so that working pressure in the chamber can be up to four orders of magnitude higher than the pressure in the FEL beamline. [doi:10.1063/1.3327816]

I. INTRODUCTION

Scattering experiments with soft x-ray radiation (2–10 nm) are ideal for studying the structure of nanosized objects, for determining the electron density shape of aperiodic systems or periodic structures of nanoensembles with lattice constants of about 5–10 nm and bigger, such as periodic self-assembled structures or macromolecular crystals.[1] Structural studies on such materials are of particular importance for the development of nanoconfined materials with new and extraordinary physical and chemical properties, in biology or in nanomedicine.[2] Recent developments of highly intense ultrashort soft x-ray radiation generated with the soft x-ray free electron lasers (FELs) (FLASH, LCLS) (Refs. 3 and 4) allows for new kind of diffraction or spectroscopic experiments[5–8] in this wavelength regime. The coupling of an optical femtosecond laser enables for ultrafast time resolved diffraction experiments with soft x-ray radiation: The optical laser excitation can be used to change the state of matter, to generate structures far away from equilibrium, or initiate chemical[9,10] or biochemical[11,12] reactions with the advantage of an initial, optically well-defined, and coherent excitation of the sample. It is also possible to use the x-ray beam to induce changes in the materials and then probe with the laser beam to monitor changes in electro-optical properties. With the possibility to insert liquid samples in a liquid jet form into vacuum,[13–17] FEL experiments are no more limited to solid and gaseous samples.

Due to the high absorbance of soft x-ray photons by air, all experiments require high vacuum conditions. The vacuum chambers have to be big enough to allow connection of all necessary equipment, e.g., sample holders and detectors. At the same time, these chambers should be as small as possible so that the downtime in the operation when they have to be vented and pumped down again is kept minimal. In this work, we present a design of a multipurpose vacuum chamber which can be used for multiple types of pump/probe measurements (optical transmission and reflection and soft x-ray diffraction) and with different kinds of samples (solid samples or liquid jet), while having a small size.

II. SETUP

The main component of the setup (Fig. 1) is an octagonal ring with an outer diameter of 210 mm and inner diameter of 160 mm [see Fig. 2(a)]. All eight sides have embedded DN40 CF flanges, while both bases have DN160 Conflat (CF) flanges. During the experiments the chamber is positioned vertically so that flange 1 is directly above flange 5.

The vacuum chamber is evacuated by an oil-free Oerlikon Leybold pump system which consists of an EcoDry M prepump and a MAG W 400 iP turbomolecular pump with a DN160 CF flange, connected directly to a DN160 CF chamber flange. Direct connection over a big flange is an important feature for the quick evacuation of the chamber. With this configuration, it is possible to pump out the vacuum chamber containing a solid sample to a pressure lower than 10^{-6} mbar in less than 20 min, which allows starting the measurement.

Flange 3 is connected to a DN40 CF cross which carries various tools: a vacuum gauge, a movable FEL x-ray beam dump, and a SMA (SubMiniature version A) vacuum feedthrough connector for an avalanche diode. This avalanche diode is sensitive in the soft x-ray as well as in the optical light range. Based on the rise time of ~100 ps it is possible to roughly determine the temporal overlap between the FLASH FEL beam and the optical laser. As another possibility to find the time zero point, flange 2 can be used to

[a)]Author to whom correspondence should be addressed. Electronic mail: stecher@gwdg.de.

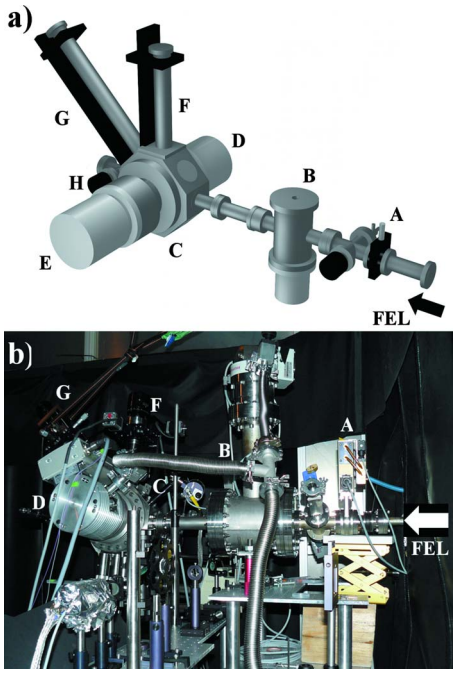

FIG. 1. (Color online) (a) 3D model of the vacuum chamber. The free electron laser (FEL) beam is coming from the right side and is passing through the vacuum shutter (A) and the differential pumping stage (B) before entering the main chamber (C). The turbomolecular vacuum pump (D) and the x-ray camera (E) are connected to the DN160 CF ports of the chamber. The sample positioning vacuum manipulator (F) is connected onto the top part, while the manipulator which holds coaxial cable holder used for time zero measurement (G) is connected next to it. After passing through the main chamber, the FEL beam enters a DN40 CF cross (H) which holds the beam stop and the vacuum gauge. (b) Photograph of the experimental setup at the FLASH beamline. The FEL beam is coming from the right side and first passes the vacuum shutter (A). The experiments shown investigated solid samples, so the differential pumping stage (B) did not use a cooling trap, and the turbomolecular vacuum pump was mounted from the upper side. The main chamber (C) has the sample positioning vacuum manipulator (F) and the coaxial cable holder (G) connected to the upper side and the turbomolecular vacuum (D) pump to the side. The optical setup used for reflectometry measurements has been installed on the optical plate next to the chamber.

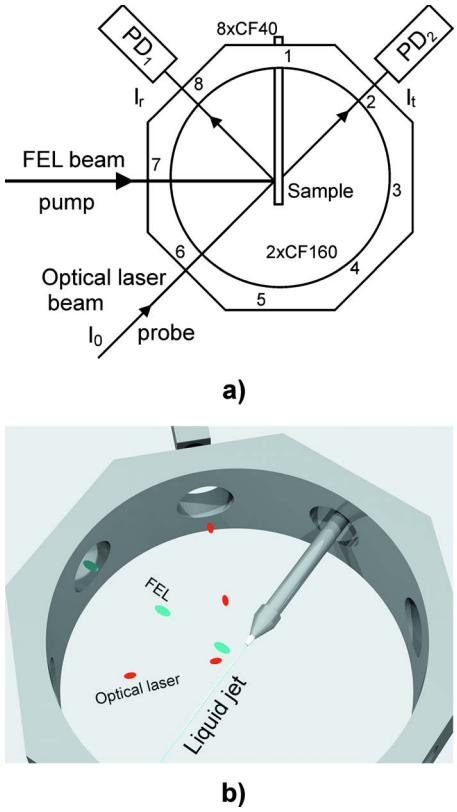

FIG. 2. (Color online) (a) Schematics of the optical reflection and optical transmission experiments. The eight DN40 CF side-flanges are labeled 1–8. The sample, which can be either a solid sample or a liquid jet, is positioned through the flange 1. The soft x-ray beam is entering the chamber through the flange 7, and the optical laser beam through the flange 6. The intensity of the reflected (I_r) and transmitted (I_t) laser beams can be measured at the flanges 8 and 2, respectively. The intensity of the optical beam I_0 is measured before entering the experimental chamber for signal normalization. (b) 3D model of the pump/probe experiments with the liquid jet. In this setup, the FEL pulses (lighter shade of gray, blue online) are used as a pump, and optical laser pulses (darker shade of gray, red online) are used as a probe in the reflection geometry. A photodiode is connected to the outside of the flange 8 and it is recording the intensity of the reflected signal. Due to the fact that laser pulses become divergent after reflection from the water jet, a convex lens can be placed between the chamber and the photodiode in order to increase the detected signal.

connect a second manipulator with a SMA coaxial cable, which is on another end connected to the oscilloscope. By using the electrical signals produced in the coaxial cable by x-ray and laser pulses, temporal overlap can be found within a 50 ps interval.[18] If it is necessary to obtain better vacuum conditions in a direction of an incoming FEL beam flange 7 can be connected to a differential pumping stage (DPS), which will be described later.

A. Solid samples

For measurements with solid samples, a motorized xyz-manipulator is mounted on flange 1. The manipulator has a 100 mm distance range on the z-axis while the movements in the xy-plane are limited by the size of the DN40 CF flange to a 40 mm diameter circle. The position can be changed remotely in all three directions by the use of a joystick or it can be computer controlled. The computer software also allows programming of various consecutive movements to be completed automatically, which is a useful tool for automatization of measurements during the destructive experiments, which demand a fresh sample for each pair of pump and probe pulses. The sample manipulator is equipped with a multisample holder that is capable of connecting up to four different samples at the same time, with the total area of 9×3.5 cm^2. The inner frame of the sample holder is also used as a holder for a metal substrate covered with photoluminescent material used for finding the spatial overlap between a FEL soft x-ray beam and an optical laser beam.

B. Liquid jet

In addition to the solid samples, liquid samples can also be studied in this chamber. They are pumped into the vacuum through a nozzle with a diameter of 5–100 μm. Experiments presented in this article were performed with 20–60 μm nozzles, while the possibility of using the smallest 5 μm nozzle was demonstrated but not yet characterized by reflection measurements like in Fig. 4. For the experiments, the xyz-manipulator is mounted on flange 1 and it is holding the liquid jet guiding pipe made out of stainless steel. Liquid is pumped into the chamber using a HPLC

pump Knauer Smartline Pump 1000. This way it is possible to set the flow rate of the liquid jet up to 10 ml/min with an accuracy better than 0.5% and to keep it constant with a precision better than 0.1%. Immediately after passing through the nozzle, the liquid has a laminar flow for a certain length, usually few millimeters.[19,20] This part of the flow can be used to perform experiments involving (dis-)ordering of different liquid samples after laser irradiation or change in their electric properties after absorbing a FEL pulse. Usually, the setup can run with these stable conditions up to 8 h, depending on the liquid jet flow rate, and that time should be sufficient for performing a time resolved measurement.

Although it is also possible to use flow-through cells for experiments with liquid in vacuum, it would be impossible to use them with the FEL radiation because the cell windows would get damaged.

On the opposite side of the liquid jet system, on flange 5, a cooling finger is installed in order to collect the liquid coming out of the liquid jet during experiments. This cooling finger is immersed in a dewer filled with liquid nitrogen so that all collected liquid is frozen in order to keep the vacuum conditions stable. The turbomolecular pump is protected from the direct flow of liquid and solvent molecules in the gas phase by a cooling trap, which is installed in the vacuum T-cross between the chamber and the pump. The trap is filled with liquid nitrogen and it collects and freezes all liquid and solvent molecules in the gas phase coming from the liquid jet toward the turbopump. The usage of the cooling trap increases the vacuum pumping speed two to five times and also helps the turbomolecular vacuum pump to reach higher rotational speed than compared to a setup without the cooling trap.

During the experiments utilizing the liquid jet, the pressure in the chamber is kept stable in the 10^{-3} mbar range. To be able to provide 10^{-7} mbar pressure on the side that is connected to the FEL, DPSs should be installed (one or two of them). Each of them consist of the vertically positioned four-way reducer vacuum cross (DN100 CF to DN40 CF), with the turbopump on the lower side of the cross and the cooling finger filled with liquid nitrogen on the upper side. With one of the DN40 CF flanges one DPS is connected to flange 7 of the chamber, and with the second DN40 CF the DPS is connected to the second DPS. In each of the DN40 CF connections a 2–10 mm aperture is installed to minimize the amount that the liquid and solvent molecules in the gas phase can pass from the chamber into the DPS and to maximize the pressure ratio between them. During the operation, liquid and solvent molecules in the gas phase which manage to go through the aperture into the DPS will be collected onto the cooling fingers, preventing them from entering the FEL vacuum pipe. The final pressure achievable at the end of the second DPS with the liquid jet running is in the lower 10^{-7} mbar range. If the required vacuum pressure is in the 10^{-6} mbar range, it can be achieved with one DPS alone. The calculation for the final pressure can be found in literature;[21] however this cannot be successfully implemented for our setup due to the inclusion of the cooling trap which significantly improves the vacuum conditions. The efficiency of a pumping stage was experimentally monitored by a vacuum gauge and, depending on the diameter of the pinhole used, the ratio of the pressure before and after the DPS was in the 10^2–10^3 range. Additionally, to ensure that no liquid or solvent molecules in the gas phase would enter the FEL tube, a test experiment was performed with the mass spectrometer connected after the DPS. During this measurement, no traces of the material coming from the liquid jet were observed. Additionally, the connections between the chamber and the DPS and between the first and second DPSs can be made with the DN40 CF flexible bellows, thus allowing for the precise placement of all the components in order to ensure that the pump beam is passing through all the apertures.

An automatic refill system for all liquid nitrogen traps in the setup has been developed. There are four cooling traps in the setup: one beneath the liquid jet, one in front of the turbopump, and two in the DPSs. Liquid nitrogen from a pressurized liquid nitrogen tank is delivered to all of them through insulated copper pipes. Each of the cooling traps is equipped with two temperature sensors that are monitoring the level of liquid nitrogen. The sensors are connected to a controller that opens and closes magnetic valves on each of the delivering copper pipes. Once the level drops below the lower sensor, the magnetic valve will automatically open the pipe delivering the liquid nitrogen to that specific cooling trap. When the liquid nitrogen level reaches the upper sensor, the magnetic valve closes.

For the reflectivity experiments, due to the fact that laser pulses become divergent after reflection from the liquid jet which acts as a convex cylindrical mirror, a convex lens can be placed between the chamber and the photodiode in order to increase the amount of the reflected signal arriving onto the photodiode.

III. EXPERIMENTS

A. Optical reflection and optical transmission experiments

When using FEL pulses as a pump to induce ultrafast changes in materials, one way of observing these changes is by probing the sample with the Ti:sapphire or Nd:YAG (yttrium aluminum garnet) laser pulses. Depending on the type of the sample (bulk solid sample, thin film, and liquid jet) and the optical properties of the material, the measured probe signal can be the transmitted, reflected, or both of them. The probe pulse is entering the chamber through flange 6. For measuring the intensity of the reflected pulses, a photodiode is mounted outside flange 8 [see Fig. 2(b)], and for the intensity of the transmitted pulses another photodiode is mounted outside flange 2. All of these flanges (2, 6, and 8) are closed by DN40 CF viewports, which are transparent for the radiation in the range between 250 and 2000 nm, which permits to use not only the fundamental wavelengths of the Ti:sapphire and Nd:YAG lasers (800 and 1064 nm, respectively) but their harmonics as well, down to 266 nm. One additional photodiode is positioned behind the last mirror in front of the chamber and it is monitoring the intensity of the probe beam before it hits the sample. The recorded intensity is used to normalize the reflected and transmitted signals.

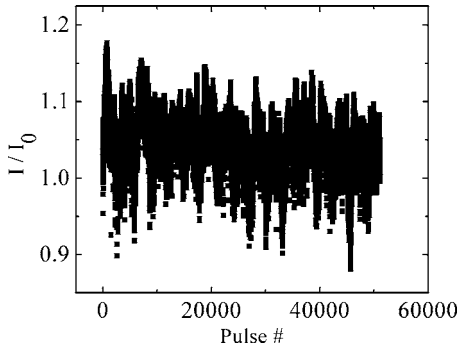

FIG. 3. Stability of the normalized reflected optical signal (100 fs and 800 nm) from the liquid jet running in vacuum. Each point represents one pulse. The standard deviation of the recorded signal is 3.5%.

Figure 3 emphasizes the stability of the setup in the reflectivity mode. It shows the intensity of the signal obtained from 100 fs, 800 nm laser pulses reflected from the running liquid jet. Although some signal instability cannot be totally avoided due to the instability of the surface of the liquid jet, the intensity distribution of the reflected signal had a standard deviation of only 3.5%, while the laser intensity had 1% standard deviation. With a sufficient number of integrated pulses for each time point in the time resolved measurement, the stability of the measured signal can be improved to less than 1%, which is adequate for monitoring structural and electro-optical changes induced in the liquid samples.

The temporal and spatial calibrations of the chamber have been performed at a home femtosecond laser source with a standard transient reflectometry setup. In Fig. 4, a typical result of this optical pump (400 nm, 300 μm focus)/optical probe (800 nm, 200 μm focus) experiment on water is presented. The nozzle diameter was 20 μm and the flow rate was 0.6 ml/min. Each of the time points is integrated over 1000 pulses. It is well known that 400 nm optical light pulses lead to the creation of solvated electrons[22] and other transient effects in water such as dielectric constant changes. These effects can be monitored by 800 nm reflectivity. The changes in the reflected intensity on the order of a percent can be easily observed, and it is possible to track changes in the change in reflectivity down to 0.05% with the temporal resolution of ~200 fs. At the time zero point, the reflected

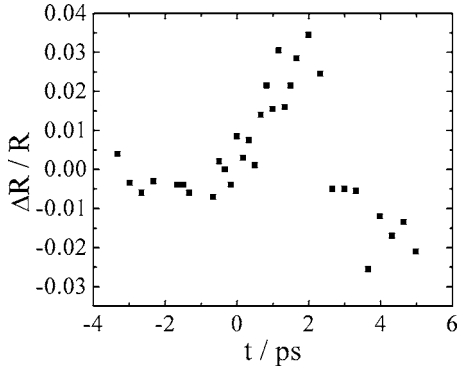

FIG. 4. Change in the reflection intensity of the laser beam from the liquid jet after the excitation by second laser beam. The wavelength of the pump beam was 400 nm and of a probe beam was 800 nm. Each time point is integrated over 1000 pulses.

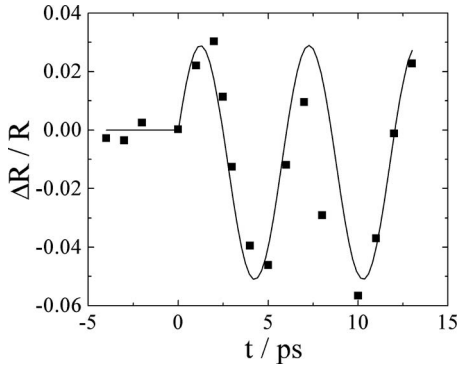

FIG. 5. Change in the reflectivity of a PMMA sample after illumination by a soft x-ray FLASH beam. The probe beam has been delivered by a Ti:sapphire optical laser at 800 nm and the FLASH soft x-ray beam had a wavelength of 8 nm.

signal has an increase in intensity with a time constant of about 1 ps followed by an intensity decay

Figure 5 shows the temporal and spatial calibration strategy for FEL pump/optical probe experiments. For this experiment, a solid sample [poly(methyl methacrylate) (PMMA)] was irradiated by the 30 fs long 8 nm soft x-ray FLASH pulses and the reflectivity changes of the 800 nm laser pulses were monitored. Here, the intensity stability is better than with the liquid jet and even the smaller changes can be resolved with the same 200 fs temporal resolution. The oscillations of the reflected signal after the laser excitation can be accurately fitted. The results of the experiments will be discussed elsewhere.

B. Soft x-ray diffraction and scattering experiments

On the second DN160 CF flange an extreme ultraviolet radiation (XUV) sensitive charge-coupled device (CCD) camera for detection of x-ray diffraction signal can be installed (Princeton Instruments, PIXIS-XO 2048 $\times$2048 pixels with a DN100 CF flange connection). In order to reduce a background in diffraction images by preventing laser light from hitting the CCD chip, a 100 nm thick palladium foil with a diameter of 40 mm was installed as a filter between the camera and the chamber. The camera is not connected directly to the flange but over a flexible bellow (DN160 CF to DN100 CF) so that horizontal camera position could be modified for $\pm$20 mm.

With this setup the changes in soft x-ray diffracted signal after the optical excitation by laser pulse can be monitored. First, in this version of the chamber, it is possible to monitor the diffracted signal at 2θ angles in the range of 80°–100° in the horizontal plane. For the currently available soft x rays in FLASH which are in the range of 7–30 nm, this determines the characteristic d-spacing of the samples to be investigated to 5–20 nm, which includes many interesting macromolecular materials, such as proteins with appropriate radii of gyration or self-assembled chemical systems, such as liquid crystals.

The chamber is positioned on two goniometers (Huber 1-Circle Segments), which can be used for rotation around

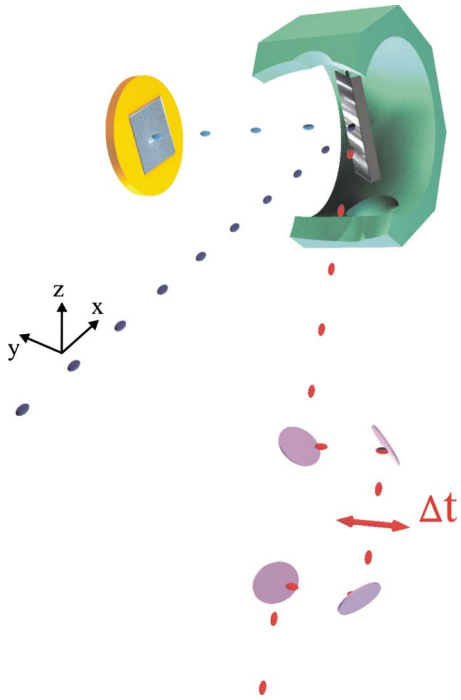

FIG. 6. (Color online) 3D model of the pump/probe setup with solid samples. The laser pulses (lighter shade of gray, red online) are used as the pump beam while the soft x-ray pulses (darker shade of gray, blue online) are used as the probe beam. In this example, the diffracted signal is monitored with the CCD camera attached on one of the DN160 CF flanges, recording the diffraction at $2\theta=90°$. By adjusting the delay stage in the path of the optical laser beam it is possible to change the relative arrival time between the pump and probe beams.

the horizontal axis defined by x-ray beam. The maximum rotation angle is 20° in both directions. This is useful for the diffraction experiments where x rays are linearly polarized and the diffracted intensity in the horizontal plane is practically zero. By rotating the whole chamber, including the connected x-ray camera, diffracted signal in the areas above or below horizontal plane can be detected.

In Fig. 6, a three-dimensional (3D) model of the diffraction experiment is shown. The laser pulses (red color) are used as the pump beam while the soft x-ray pulses (blue color) are used as the probe beam. The diffracted signal is monitored with the CCD camera attached on one of the DN160 CF flanges, recording the diffracted signal at $2\theta=90°\pm4°$. By adjusting the delay stage in the path of the laser beam, it is possible to change the relative arrival time between pump and probe pulses.

A Bragg diffraction spot from a single crystal silver behenate sample and the diffraction ring from the polycrystalline sample are presented in Figs. 7(a) and 7(b), respectively. Both images are obtained using 8 nm wavelength 30 fs long soft x-ray pulses from FLASH, focused to ~200 μm on the sample plane. The Bragg reflection is recorded with only one FLASH pulse, while the polycrystalline signal is integrated over four pulses in this experiment. Silver behenate has a well-defined structure[23] and its diffraction can be used as a standard reference for diffraction experiments at soft x-ray sources.

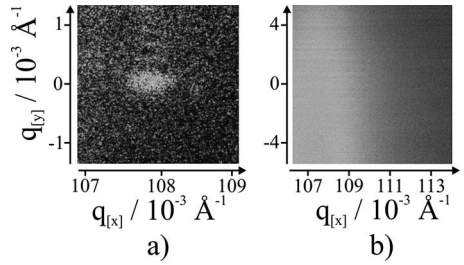

FIG. 7. Diffraction from a silver behenate sample using the FLASH soft x rays with 8 nm wavelength. (a) Diffraction from the single crystalline sample. The image has been recorded in a single pulse mode. (b) The powder diffraction signal from the polycrystalline silver behenate sample. The final image was accumulated over four pulses. The vertical stripe is a part of a diffraction ring with 2θ angle of 86.5°.

IV. CONCLUSION

We have built a compact and easily extendable vacuum chamber for versatile experiments with FEL radiation. Its small size is especially convenient for fast allocation to different experimental facilities. Although its primal function is to be used in experiments involving FEL radiation, it can be used for any reflection/transmission/diffraction experiments with high vacuum requirement. With multiple CF flange ports available, many other radiation sources and detectors can be easily connected. Having a small volume, it can quickly reach the operational vacuum conditions; nonetheless, there is enough space for mounting and manipulating multiple samples simultaneously. The jet system provides the means for serial experiments, such as serial diffraction and serial spectroscopy, where rapid exchange of samples is required.

ACKNOWLEDGMENTS

This work was supported by SFB 602 and SFB 755 of the Deutsche Forschungsgemeinschaft. Furthermore, S.T. is grateful to the DFG (Grant No. TE347, 1-3), Aventis Foundation, Fonds of the Chemical Industry and EU-FLASH MC-8041. The authors would like to thank R. Treusch, S. Duesterer, and A. Foehlisch for their helpful discussions and the Max Planck Advanced Study Group for their continuous support. I. Rajkovic and J. Hallmann contributed equally in this work.

[1] A. Guinier, *X-ray Diffraction in Crystals, Imperfect Crystals, and Amorphous Bodies* (Dover, New York, 1963).
[2] A. S. F. Ramos and S. Techert, Biophys. J. **89**, 1990 (2005).
[3] E. L. Saldin, E. A. Schneidmiller, and M. Yurkov, *The Physics of Free-Electron Lasers* (Springer, Berlin, 2000).
[4] W. Ackermann, G. Asova, V. Ayvazyan, A. Azima, N. Baboi, J. Bahr, V. Balandin, B. Beutner, A. Brandt, A. Bolzmann, R. Brinkmann, O. I. Brovko, M. Castellano, P. Castro, L. Catani, E. Chiadroni, S. Choroba, A. Cianchi, J. T. Costello, D. Cubaynes, J. Dardis, W. Decking, H. Delsim Hashemi, A. Delserieys, G. Di Pirro, M. Dohlus, S. Dusterer, A. Eckhardt, H. T. Edwards, B. Faatz, J. Feldhaus, K. Flottmann, J. Frisch, L. Frohlich, T. Garvey, U. Gensch, C. Gerth, M. Gorler, N. Golubeva, H. J. Grabosch, M. Grecki, O. Grimm, K. Hacker, U. Hahn, J. H. Han, K. Honkavaara, T. Hott, M. Huning, Y. Ivanisenko, E. Jaeschke, W. Jalmuzna, T. Jezynski, R. Kammering, V. Katalev, K. Kavanagh, E. T. Kennedy, S. Khodyachykh, K. Klose, V. Kocharyan, M. Korfer, M. Kollewe, W. Koprek, S. Korepanov, D. Kostin, M. Krassilnikov, G. Kube, M. Kuhlmann, C. L. S. Lewis, L. Lilje, T. Limberg, D. Lipka, F. Lohl, H. Luna, M. Luong, M. Martins, M. Meyer, P. Michelato, V. Miltchev, W. D. Moller, L. Monaco,

W. F. O. Muller, O. Napieralski, O. Napoly, P. Nicolosi, D. Nolle, T. Nunez, A. Oppelt, C. Pagani, R. Paparella, N. Pchalek, J. Pedregosa Gutierrez, B. Petersen, B. Petrosyan, G. Petrosyan, L. Petrosyan, J. Pfluger, E. Plonjes, L. Poletto, K. Pozniak, E. Prat, D. Proch, P. Pucyk, P. Radcliffe, H. Redlin, K. Rehlich, M. Richter, M. Roehrs, J. Roensch, R. Romaniuk, M. Ross, J. Rossbach, V. Rybnikov, M. Sachwitz, E. L. Saldin, W. Sandner, H. Schlarb, B. Schmidt, M. Schmitz, P. Schmuser, J. R. Schneider, E. A. Schneidmiller, S. Schnepp, S. Schreiber, M. Seidel, D. Sertore, A. V. Shabunov, C. Simon, S. Simrock, E. Sombrowski, A. A. Sorokin, P. Spanknebel, R. Spesyvtsev, L. Staykov, B. Steffen, F. Stephan, F. Stulle, H. Thom, K. Tiedtke, M. Tischer, S. Toleikis, R. Treusch, D. Trines, I. Tsakov, E. Vogel, T. Weiland, H. Weise, M. Wellhofer, M. Wendt, I. Will, A. Winter, K. Wittenburg, W. Wurth, P. Yeates, M. V. Yurkov, I. Zagorodnov, and K. Zapfe, Nat. Photonics **1**, 336 (2007).

[5] H. N. Chapman, A. Barty, M. J. Bogan, S. Boutet, M. Frank, S. P. Hau-Riege, S. Marchesini, B. W. Woods, S. Bajt, H. Benner, R. A. London, E. Plonjes, M. Kuhlmann, R. Treusch, S. Dusterer, T. Tschentscher, J. R. Schneider, E. Spiller, T. Moller, C. Bostedt, M. Hoener, D. A. Shapiro, K. O. Hodgson, D. Van der Spoel, F. Burmeister, M. Bergh, C. Caleman, G. Huldt, M. M. Seibert, F. R. N. C. Maia, R. W. Lee, A. Szoke, N. Timneanu, and J. Hajdu, Nat. Phys. **2**, 839 (2006).

[6] P. Coppens, I. Novozhilova, and A. Kovalevsky, Chem. Rev. (Washington, D.C.) **102**, 861 (2002).

[7] C. Gahl, A. Azima, M. Beye, M. Deppe, K. Dobrich, U. Hasslinger, F. Hennies, A. Melnikov, M. Nagasono, A. Pietzsch, M. Wolf, W. Wurth, and A. Fohlisch, Nat. Photonics **2**, 165 (2008).

[8] S. P. Hau-Riege, R. A. London, H. N. Chapman, A. Szoke, and N. Timneanu, Phys. Rev. Lett. **98**, 198302 (2007).

[9] G. Busse, T. Tschentscher, A. Plech, M. Wulff, B. Frederichs, and S. Techert, Faraday Discuss. **122**, 105 (2003).

[10] A. Jung, T. Domratcheva, M. Tarutina, Q. Wu, W. H. Ko, R. L. Shoeman, M. Gomelsky, K. H. Gardner, and L. Schlichting, Proc. Natl. Acad. Sci. U.S.A. **102**, 12350 (2005).

[11] E. Collet, M. H. Lemee-Cailleau, M. Buron-Le Cointe, H. Cailleau, M. Wulff, T. Luty, S. Y. Koshihara, M. Meyer, L. Toupet, P. Rabiller, and S. Techert, Science **300**, 612 (2003).

[12] X. Yang, E. A. Stojkovic, J. Kuk, and K. Moffatt, Proc. Natl. Acad. Sci. U.S.A. **104**, 12571 (2007).

[13] A. Charvat, E. Lugovoj, M. Faubel, and B. Abel, Eur. Phys. J. D **20**, 573 (2002).

[14] A. Charvat, E. Lugovoj, M. Faubel, and B. Abel, Rev. Sci. Instrum. **75**, 1209 (2004).

[15] R. Weber, B. Winter, P. M. Schmidt, W. Widdra, I. V. Hertel, M. Dittmar, and M. Faubel, J. Phys. Chem. B **108**, 4729 (2004).

[16] B. Winter, M. Faubel, I. V. Hertel, C. Pettenkofer, S. E. Bradforth, B. Jagoda-Cwiklik, L. Cwiklik, and P. Jungwirth, J. Am. Chem. Soc. **128**, 3864 (2006).

[17] B. Winter, R. Weber, W. Widdra, M. Dittmar, M. Faubel, and I. V. Hertel, J. Phys. Chem. A **108**, 2625 (2004).

[18] A. Foelisch, personal communication (2008).

[19] C. Weber, Z. Angew. Math. Mech. **11**, 136 (1931).

[20] M. Goldin, J. Yerushal, R. Pfeffer, and R. Shinnar, J. Fluid Mech. **38**, 689 (1969).

[21] R. Jackel, *Kleinste Drucke, ihre Messung und Erzeungung* (Springer, New York, 1950), pp. 265–273.

[22] J. L. McGowen, H. M. Ajo, J. Z. Zhang, and B. J. Schwartz, Chem. Phys. Lett. **231**, 504 (1994).

[23] T. C. Huang, H. Toraya, T. N. Blanton, and Y. Wu, J. Appl. Crystallogr. **26**, 180 (1993).